Supplemental Data

Supplemental Table s1

Electrical stimulation parameters

Voltage (V)	Ampere (A)
0	—
5	0.01±0.00
10	0.57±0.00
20	1.46±0.00

All values are means ± s.e.m. (n = 5).

Supplemental Table s2

Embryos derived from blastocysts receiving EB or EP injections

	11 dpc			13 dpc			11 dpc+13 dpc		
	dorsal[1]	other[2]	total[3]	dorsal	other	total[3]	dorsal	other	total
EP[4]	4	2	9	3	1	4	7	3	13
EB[5]	0	3[6]	10	0	1	5	0	4	15

[1]Number of embryos containing fluorescent cells that incorporated primarily to dorsal structures (CNS).

[2]Number of embryos containing fluorescent cells that incorporated primarily into non-dorsal structures.

[3]Total number of recovered embryos with or without fluorescent cells.

[4,5]EP and EB represent stimulated and non-stimulated EBs, respectively.

[6]Two of the three embryos have fluorescent only in yolk sac.

Supplemental Figure Legends

Figure s1. The majority of cells derived from EBs receiving 10-V stimulation express MAP2 but not GFAP: 97.5% (117/120) of cells counted from four random fields in the microscope were MAP2 immunoreactive. Scale bar, 50 μm.

Figure s2. Whole mounted mouse embryos injected with electrically stimulated or non-stimulated EBs. Upper and lower panels show 11 dpc and 13 dpc embryos, respectively. Embryos on the left side of each panel were injected with stimulated EBs, whereas those on the right side were injected with non-stimulated EBs. One 11 dpc embryos of non stimulated EB showed developmental abnormality, while all 10 embryos recieved EP derived cells are morphologically normal.

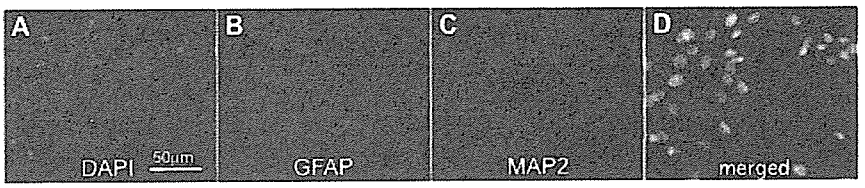

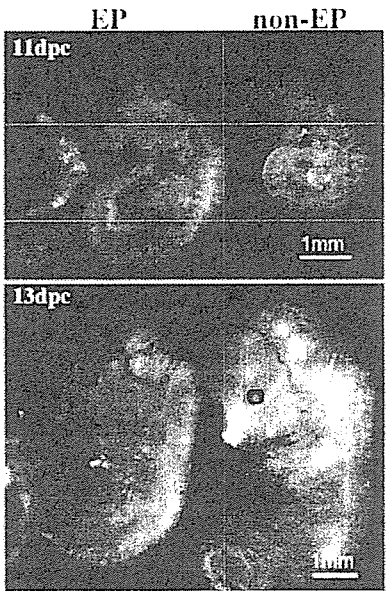

Electrical stimulation modulates fate determination of differentiating embryonic stem cells

Masahisa Yamada, Kentaro Tanemura, Seiji Okada, Akio Iwanami, Masaya Nakamura, Hideaki Mizuno, Michiru Ozawa, Ritsuko Ohyama-Goto, Naohito Kitamura, Masako Kawano, Kyoko Tan-Takeuchi, Chiho Ohtsuka, Atsushi Miyawaki, Akihiko Takashima, Masaharu Ogawa, Yoshiaki Toyama, Hideyuki Okano and Takashi Kondo

Stem Cells published online Nov 16, 2006;
DOI: 10.1634/stemcells.2006-0011

Journal of Neurochemistry, 2006, **99**, 277–287 doi:10.1111/j.1471-4159.2006.04033.x

Failure to support a genetic contribution of *AKT1* polymorphisms and altered AKT signaling in schizophrenia

Masayuki Ide,*,† Tetsuo Ohnishi,* Miyuki Murayama,‡ Izuru Matsumoto,§ Kazuo Yamada,* Yoshimi Iwayama,* Irina Dedova,§,¶ Tomoko Toyota,* Takashi Asada,† Akihiko Takashima‡ and Takeo Yoshikawa*,**

**Laboratory for Molecular Psychiatry, and ‡Laboratory for Alzheimer's Disease, RIKEN Brain Science Institute, Saitama, Japan*

†Department of Psychiatry, University of Tsukuba School of Medicine, Ibaraki, Japan

§Department of Pathology, University of Sydney & NSW, Australia

¶Neuroscience Institute of Schizophrenia and Allied Disorders, Sydney, Australia

***CREST, Japan Science and Technology Agency, Saitama, Japan*

Abstract

The protein kinase v-akt murine thymoma viral oncogene homolog (AKT) gene family comprises three human homologs that phosphorylate and inactivate glycogen synthase kinase 3β (GSK3β). Studies have reported the genetic association of *AKT1* with schizophrenia. Additionally, decreased AKT1 protein expression and the reduced phosphorylation of GSK3β were reported in this disease, leading to a new theory of attenuated AKT1-GSK3β signaling in schizophrenia pathogenesis. We have evaluated this theory by performing both genetic and protein expression analyses. A family based association test of *AKT1* did not show association with schizophrenia in Japanese subjects. The expression levels of total AKT, AKT1 and phosphorylated GSK3β detected in the schizophrenic brains from two different brain banks also failed to support the theory. In addition, no attenuated AKT-GSK3β signaling was observed in the lymphocytes from Japanese schizophrenics, contrasting with previous findings. Importantly, we found that the level of phosphorylated GSK3β at Ser9 tended to be inversely correlated with postmortem intervals, and that the phosphorylation levels of AKT were inversely correlated with brain pH, issues not assessed in the previous study. These data introduce a note of caution when estimating the phosphorylation levels of GSK3β and AKT in postmortem brains. Collectively, this study failed to support reduced signaling of the AKT-GSK3β molecular cascade in schizophrenia.

Keywords: association, glycogen synthase kinase 3β, lymphocytes, phosphorylation, postmortem brain, western blot.

J. Neurochem. (2006) **99**, 277–287.

Schizophrenia is a major psychiatric disease with a worldwide prevalence of approximately 1%. Although the pathogenesis of schizophrenia is largely unknown, the neurodevelopmental hypothesis of schizophrenia is widely accepted. It suggests that pathophysiological changes in schizophrenia start in the early neurodevelopmental period (Weinberger 1996). Based on this, the expression of neurotrophic and transcription factors, protein kinases and other molecules associated with neural development have been studied, with some proteins and transcripts showing altered expression levels in the postmortem brains of schizophrenics (Barbeau *et al.* 1995; Impagnatiello *et al.* 1998; Takahashi *et al.* 2000; Ilia *et al.* 2002; Ohnuma *et al.* 2003; Aoki-Suzuki *et al.* 2005).

AKT (also known as protein kinase B) defines a family of closely related, highly conserved cellular homologs with protein kinase activity. Three family members, AKT1, AKT2 and AKT3, have been identified in humans. They play an important role in neuronal survival and differentiation (Conti

Received April 25, 2006; revised manuscript received May 31, 2006; accepted June 1, 2006.

Address correspondence and reprint requests to Takeo Yoshikawa MD PhD, Laboratory for Molecular Psychiatry, RIKEN Brain Science Institute, 2–1 Hirosawa, Wako-city, Saitama 351–0198, Japan. E-mail: takeo@brain.riken.go.jp

Abbreviations used: BA, Brodmann's area; ETDT, extended transmission disequilibrium test; GSK3β, glycogen synthase kinase 3β; LD, linkage disequilibrium; NSW, TRC, New South Wales Tissue Resource Center; PBS-T, phosphate-buffered saline with 0.05% Tween 20; PDT, pedigree disequilibrium test; PMI, postmortem interval; PP2A, protein phosphatase 2A; SDS, sodium dodecyl sulfate; SNP, single nucleotide polymorphism.

et al. 2001; Dudek *et al.* 1997). Moreover, these enzymes mediate intracellular signaling for axon elongation and branching (Markus *et al.* 2002). Phosphorylated AKT inactivates glycogen synthase kinase 3β (GSK3β) through phosphorylation at the Ser9 site (Cross *et al.* 1995). GSK3β mediates apoptotic signals either by inhibiting transcription factors or by degrading β-catenin. Perturbation of this GSK3β pathway may mediate the pathogenesis of neurodegenerative disorders and schizophrenia (Kozlovsky *et al.* 2002; De Ferrari *et al.* 2003). Kozlovsky *et al.* (2000, 2004) reported decreased expression levels of GSK3β protein and mRNA in postmortem brains from schizophrenic patients. Beaulieu *et al.* (2004) showed a functional link between the AKT-GSK3β signaling pathway and increased dopaminergic neurotransmission, another putative etiologic factor in schizophrenia.

Emamian *et al.* (2004) demonstrated that protein expression of AKT1 and phosphorylation levels of GSK3β at Ser9 were reduced in postmortem brains and Epstein–Barr virus-transformed lymphocytes from schizophrenic patients. They showed that *AKT1* polymorphisms were associated with schizophrenia, and that subjects with a core risk haplotype had a lower expression of AKT1 in lymphocytes relative to subjects with a common haplotype. In mouse experiments, treatment with the typical neuroleptic haloperidol resulted in the up-regulation of phosphorylated AKT1 (active) and phosphorylated GSK3β at Ser9 (inactive) in the brain.

Tau is a microtubule-associated protein and another target of GSK3β (Morishima-Kawashima *et al.* 1995). Beffert *et al.* (2002) reported that reelin signaling, another system implicated in schizophrenia, suppressed tau protein phosphorylation through the activation of AKT and the inactivation of GSK3β. Therefore, impairment of AKT activity *in vivo* would be reflected in the enhanced levels of phosphorylated tau protein. In this study we aimed to extend previous reports by re-examining the AKT-GSKβ cascade and tau phosphorylation levels in schizophrenia and other mental disorders, performing protein expression analyses in postmortem brains and lymphocytes obtained from patients, and by undertaking a genetic association study between *AKT1* and schizophrenia.

Materials and methods

Subjects for the family based association study

Families with a genetic predisposition for schizophrenia for the family based association study were recruited from a geographic area located in central Japan. The probands, both in- and outpatients, were followed up by hospital doctors for at least 6 months. The sample consisted of 124 families with 376 members, of whom 163 suffered from schizophrenia. These included: (i) 80 independent and complete trios (schizophrenic offspring and their parents); (ii) 15 probands with one affected parent; (iii) 13 probands with affected siblings; (iv) 30 probands with discordant siblings (for detailed information see Yamada *et al.* 2004). Consensual diagnosis was made according to the DSM-IV (1994) criteria by at least two experienced psychiatrists on the basis of direct interviews, available medical records and information from hospital staff and relatives. None of the patients had additional Axis-I disorders, as defined by DSM-IV, and none of the present family members suffered from neurodegenerative disorders, including Parkinson's and Alzheimer's diseases. The present study was approved by the ethics committee of RIKEN. All subjects gave informed written consent to participate in the study after the provision and explanation of study protocols and purposes.

SNP genotyping of *AKT1*

Genomic DNA was isolated from blood samples using a standard method. We genotyped five single nucleotide polymorphisms (SNPs) at the *AKT1* locus described in the original report (Emamian *et al.* 2004). *AKT1* consists of 16 exons, and SNP1 (rs3803300), SNP2 (rs1130214), SNP3 (rs3730358), SNP4 (rs2498799) and SNP5 (rs2494732) are located in intron 2, intron 3, intron 5, exon 11 and intron 13, respectively. Assays-by-Design SNP genotyping products and TaqMan assay methods (Applied Biosystems, Foster City, CA, USA) were used to score the SNPs. Genotypes were determined using an ABI7900 sequence detection system and SDS v2.2 software (Applied Biosystems). Each marker was checked for allele-inheritance inconsistency within a pedigree with PEDCHECK software, http://watson.hgen.pitt.edu/register (O'Connell and Weeks 1998), and either conflicts or flagged alleles were resolved by re-genotyping.

Statistical analyses of genetic association

Transmission distortions in the family panel were evaluated using the pedigree disequilibrium test (PDT) (Martin *et al.* 2000) (PDT ANALYSIS PROGRAM v5.1; http://www.chg.duke.edu/software/pdt.html) and extended transmission disequilibrium test (ETDT) (Sham and Curtis 1995; http://www.mds.qmw.ac.uk/statgen/dcurtis/software.html). TRANSMIT software (Clayton 1999; http://watson.hgen.pitt.edu/docs/transmit.html) was run as a global test of haplotype transmission. Genomic linkage disequilibrium (LD) patterns retained in the Japanese population were determined by pairwise LD examination of markers within *AKT1* in 186 unrelated individuals from our schizophrenic pedigree panel. The standardized disequilibrium coefficient (D') and the squared correlation coefficient (r^2) were calculated with COCAPHASE software (http://www.mrc-bsu.cam.ac.uk/personal/frank/software/unphased/) (Dudbridge 2003).

Samples for protein analyses

The postmortem brain samples of Brodmann's area (BA) 9 (frontal cortex) and anterior hippocampus were obtained from the New South Wales Tissue Resource Centre (NSW TRC), University of Sydney, Australia. The samples were divided into two cohorts. The first cohort comprised 10 pairs of BA9 samples, and the second cohort consisted of eiht pairs of BA9 and 14 pairs of hippocampus samples. Each pair consisted of a schizophrenic patient (including one schizoaffective patient, pair no. 7 in Table 1) and a non-psychiatric control subject matched for age and sex. Detailed demographic data is shown in Table 1. Clinical information was collected in a standardized manner for use with the Diagnostic Instrument for Brain Studies (DIBS) (Keks *et al.* 1999).

Table 1 Demographic data of NSW samples

	Schizophrenic patients					Control subjects					Provided brain region	
Pair No.	Sex	Age (years)	PMI (h)	pH	Ethnicity	Sex	Age (years)	PMI (h)	pH	Ethnicity	BA9*	HPC*
1	M	57	48	6.7	Cauc/Aus	M	56	24	6.5	Cauc/Aus	Yes	Yes
2	M	40	21.5	6.2	Cauc/Aus	M	37	21	–	Cauc/Aus	Yes	Yes
3	F	58	19	6.1	Cauc/Aus	F	56	23	6.7	Cauc/Aus	Yes	Yes
4	M	32	26	6.2	Cauc/Aus	M	37	24	6.4	Cauc/Aus	Yes	Yes
5	M	30	24	6.6	Cauc/Aus	M	34	21	6.7	Cauc/Aus	Yes	Yes
6	M	57	18	6.6	Cauc/Aus	M	53	16	6.8	Cauc/Aus	Yes	Yes
7	F	61	17	6.4	Cauc/Aus	F	60	21	6.8	Cauc/Aus	Yes	Yes
8	M	52	9	6.1	Cauc/Aus	M	57	20	5.9	Cauc/Aus	Yes	Yes
9	F	56	39	6.6	Cauc/Aus	F	52	10	5.8	Cauc/Aus	Yes	Yes
10	M	44	27	6.6	Cauc/Aus	M	44	50	6.6	Cauc/Aus	Yes	Yes
11	F	67	27	6.2	Cauc/Aus	F	68	9	–	Cauc/Aus	Yes	Yes
12	M	67	5	6.4	No info	M	69	16	6.6	Cauc/Aus	Yes	No
13	M	57	36	6.4	Cauc/Aus	M	56	37	6.8	Cauc/Aus	Yes	No
14	M	50	36	6.2	Cauc/Aus	M	50	19	6.3	Cauc/Aus	No	Yes
15	F	66	13	6.5	Cauc/Aus	F	78	37	6.5	Cauc/Aus	Yes	Yes
16	M	51	21	6.0	Cauc/Aus	M	57	18	6.6	Cauc/Aus	Yes	No
17	M	27	33	6.3	Cauc/Aus	M	28	28	–	Cauc/Aus	Yes	No
18	F	67	21	6.4	Cauc/Aus	F	66	6	4.5	Cauc/Aus	Yes	Yes
Mean		52.2	24.5	6.36			53.2	22.2	6.37			
SD		12.8	10.9	0.21			13.2	10.7	0.60			

*BA9 samples are divided into two cohorts. Pairs No.1–10 comprise the first cohort and No.11–18 the second cohort. All hippocampal samples are included in the second cohort. Aus, Australian; BA, Brodmann's area; Cauc, Caucasian; F, female; HPC, hippocampus; M, male; PMI, postmortem interval.

An independent set of postmortem brain samples of BA6 (frontal cortex) from 60 subjects were obtained from the Stanley Medical Research Institute: the set comprised patients with schizophrenia, bipolar disorder, severe depression and non-psychiatric comparison subjects (Table 2). Two senior psychiatrists established DSM-IV diagnoses using information from all available medical records and from family interviews. Details regarding subject selection, diagnostic procedures and tissue processing are described elsewhere (Torrey *et al.* 2000). Data from BA6 were collected by an investigator blind to diagnosis. All samples were stored at −80°C until use.

The lymphocytes isolated from peripheral blood were obtained from schizophrenia, bipolar disorder and non-psychiatric control subjects. Each disease set comprised seven patients and these were compared with seven control subjects recruited from central Japan. Lymphocytes were transformed by the Epstein–Barr virus in a standard manner. We cultured immortalized lymphocytes in RPMI1640 media (SIGMA, St Louis, MO, USA) supplemented with 20% fetal bovine serum (Invitrogen, Carlsbad, CA, USA) and penicillin-streptomycin (Invitrogen). We used confluent cultures of lymphoblastocytes in our experiments.

Western blot analysis

Either postmortem brain tissue or lymphocytes were homogenized in ice-cold lysis buffer [20 mM Tris-HCl (pH 7.5), 150 mM NaCl and 0.5 mM EGTA] containing protease inhibitors (0.5 mM phenylmethylsulfonyl fluoride, 2 μg/mL aprotinin and 10 μg/mL leupeptin) and phosphatase inhibitors (5 mM NaF, 50 mM Na_3VO_4 and 1 μM okadaic acid). Lysates were ultracentrifuged at 4°C for 20 min

Table 2 Demographic summary of Stanley brain samples

	Schizophrenia	Bipolar disorder	Depression	Control
Sex and number	M = 8, F = 5	M = 7, F = 6	M = 9, F = 5	M = 9, F = 6
Age (years)*	43.2 ± 13.3	40.3 ± 11.3	47.6 ± 8.7	48.1 ± 10.7
Antipsychotics*,**	376 000 ± 65 000	19 000 ± 23 000		
pH*	5.92 ± 0.26	6.21 ± 0.23	6.19 ± 0.22	6.27 ± 0.24
PMI (h)*	27.7 ± 13.4	33.1 ± 16.9	26.1 ± 9.6	23.7 ± 9.9

*Values are indicated as mean ± SD; **Lifetime neuroleptic dose in fluphenazine equivalent dose.

at 1.1×10^5 g. The supernatants were assayed for total protein concentration by Lowry's method, and concentrations were equalized with lysis buffer. Supernatants were diluted with either 2 × or 3 × sodium dodecyl sulfate (SDS) sample buffer and boiled for 3 min. Samples were separated on 12% SDS-polyacrylamide gels and transferred to polyvinylidene difluoride membranes. The membranes were incubated for at least 1 h in blocking solution containing 5% skimmed milk in phosphate-buffered saline with 0.05% Tween 20 (PBS-T) and then incubated overnight at 4°C with primary antibodies in the blocking solution. After that, the membranes were washed in PBS-T.

As conventional chemiluminescent western blotting was not sensitive enough to detect phospho-GSK3β, an alkaline phosphatase-conjugated secondary antibody (Promega, Madison, WI, USA) was used for detecting all proteins of interest in the first NSW TRC cohort and GSK3β and phospho-GSK3β in the Stanley bank cohort. The signals were developed using nitro-blue tetrazolium chloride-5-bromo-4-chloro-3′-indolylphosphatase *p*-toluidine salt reagent (Nacalai tesque, Kyoto, Japan) and signal intensities were quantified using NIH IMAGE software (http://rsb.info.nih.gov/nih-image).

The other proteins of interest in the Stanley bank cohort were detected using conventional chemiluminescence, probing with either horseradish peroxydase-conjugated anti-mouse or rabbit IgG as a secondary antibody, and then visualizing the signal with either the ECL western blotting detection system (GE Healthcare Bio-Sciences, Piscataway, NJ, USA) or SuperSignal reagent (Pierce, Rockford, IL, USA), according to the manufacturer's instructions. Chemiluminescent signals were detected by an image analyzer LAS-1000 (Fujifilm, Tokyo, Japan) and quantified by IMAGE GAUGE.

In the second NSW TRC cohort we used standard-sized gels (15 cm × 13.5 cm) to load larger quantities of proteins (20 μg of protein equivalents in each well), and all antibodies, except the antibodies for tubulin and GSK3β, were diluted in Can Get Signal reagent (Toyobo, Osaka, Japan), which can enhance the antigen–antibody reaction. The signals were quantified as stated above.

Antibodies used for western blot analysis were: anti-Akt (1 : 1000; Cell Signaling, Danvers, MA, US), recognizing all AKT isoforms; anti-Akt1 (1 : 500; Upstate Biotechnology, Lake Placid, NY, USA), specific for the AKT1 isoform; anti-phospho-AKT (Ser473; 1 : 1000; Cell Signaling); anti-GSK3β (1 : 2500; BD Biosciences, San Jose, CA, US); anti-phospho-GSK3β (Ser9; 1 : 1000; Cell Signaling), anti-Tau (pS199; 1 : 2500; Biosource International, Camarillo, CA, USA), anti-Tau (pS396; 1 : 2500; Biosource International); anti-α-tubulin (1 : 25 000; Sigma). Tau-C, a purified rabbit polyclonal antibody against the C-terminal of tau protein, was used to detect whole tau (Ishiguro *et al.* 1995; Sato *et al.* 2002).

Statistical analyses for expression comparisons

The statistical significance of expression levels among groups was calculated by either the Wilcoxon signed-rank test (for paired samples) or the Mann–Whitney *U*-test, two-tailed (for unpaired samples). The statistical significance of correlation was evaluated by the Spearman's rank correlation test. We excluded one sample pair (pair no. 8 in Table 1) from the first NSW TRC cohort from the Wilcoxon signed-rank test because of an outlier with extremely low tubulin expression. However, we included this pair in the correlation test.

Results

Association analysis between *AKT1* and Japanese families with a predisposition to schizophrenia

Linkage disequilibrium examination showed strong LD between SNP1 and 2, and SNP3, 4 and 5 (Table 3). Emamian *et al.* (2004) reported marginally significant transmission distortion of one SNP, SNP3 ($p = 0.05$), which was in strong LD with SNP4 ($D' = 0.90$), as seen in our samples, and detected significant, albeit modest, global haplotypic associations ($p = 0.02$–0.05) with those haplotypes that combined SNP3 with neighboring SNPs. We examined the

Table 3 Pairwise marker-to-marker linkage disequilibrium (LD) statistics for the *AKT1* locus

	SNP1	SNP2	SNP3	SNP4	SNP5
SNP1	–	**0.956**	0.286	0.340*	0.218
SNP2	**0.218**	–	0.078	0.145	0.376*
SNP3	0.010	0.003	–	**0.897**	**1.000**
SNP4	0.073	0.003	0.094	–	**1.000**
SNP5	0.034	0.015	0.055	**0.457**	–

For each pair of markers, standardized D' is shown above the diagonal and r^2 below the diagonal. $D' > 0.8$ and $r^2 > 0.1$ are shown in gray.

Table 4 Results of the family based association study between *AKT1* and schizophrenia

	PDT *p*-value*		ETDT	Haplotype transmission (global *p*-value**)				
	SUM	AVE	*p*-value	1SNP	2SNPs	3SNPs	4SNPs	5SNPs
SNP1	0.87	0.81	0.30	0.30	0.52			
SNP2	0.76	0.63	0.88	0.89	0.29	0.33	0.54	
SNP3	0.45	0.28	0.30	0.22	0.29	0.50	0.78	0.70
SNP4	0.54	0.32	0.13	0.11	0.26	0.41		
SNP5	0.93	0.69	0.35	0.29				

*The PDT program computes two statistical measures, PDT-SUM and PDT-AVE. Briefly, PDT-SUM gives more weight to larger families, whereas PDT-AVE places equal weight on all families.
**p-values for multiallele testing. ETDT, extended transmission disequilibrium test; PDT, pedigree disequilibrium test.

same five SNPs in Japanese families with a predisposition to schizophrenia, but none of the SNPs exhibited significant transmission disequilibrium either by PDT (for all families) or by ETDT (for 80 independent and complete trios) (Table 4). Moreover, haplotype transmission analysis found no SNP-based haplotypes that were preferentially transmitted to schizophrenics (Table 4).

AKT signaling in lymphocytes from patients with schizophrenia and bipolar disorder

Emamian *et al.* (2004) reported that expression levels of AKT1 and GSK3β phosphorylated at Ser9 were both dramatically decreased to less than 50% in cultured lymphocytes from schizophrenic patients. We performed western blotting to examine these potential alterations of AKT signaling in cultured lymphocytes obtained from both schizophrenic patients and patients with bipolar disorder. β-Actin was used as an internal control because the expression of tubulin (used in the study of Emamian *et al.* 2004) in lymphocytes varied widely among the samples (data not shown). The lymphocyte expression of AKT and GSK3β was unaltered in schizophrenia and bipolar disorder samples relative to controls (Figs 1a, b and e). Furthermore, no significant differences were found in the phosphorylation

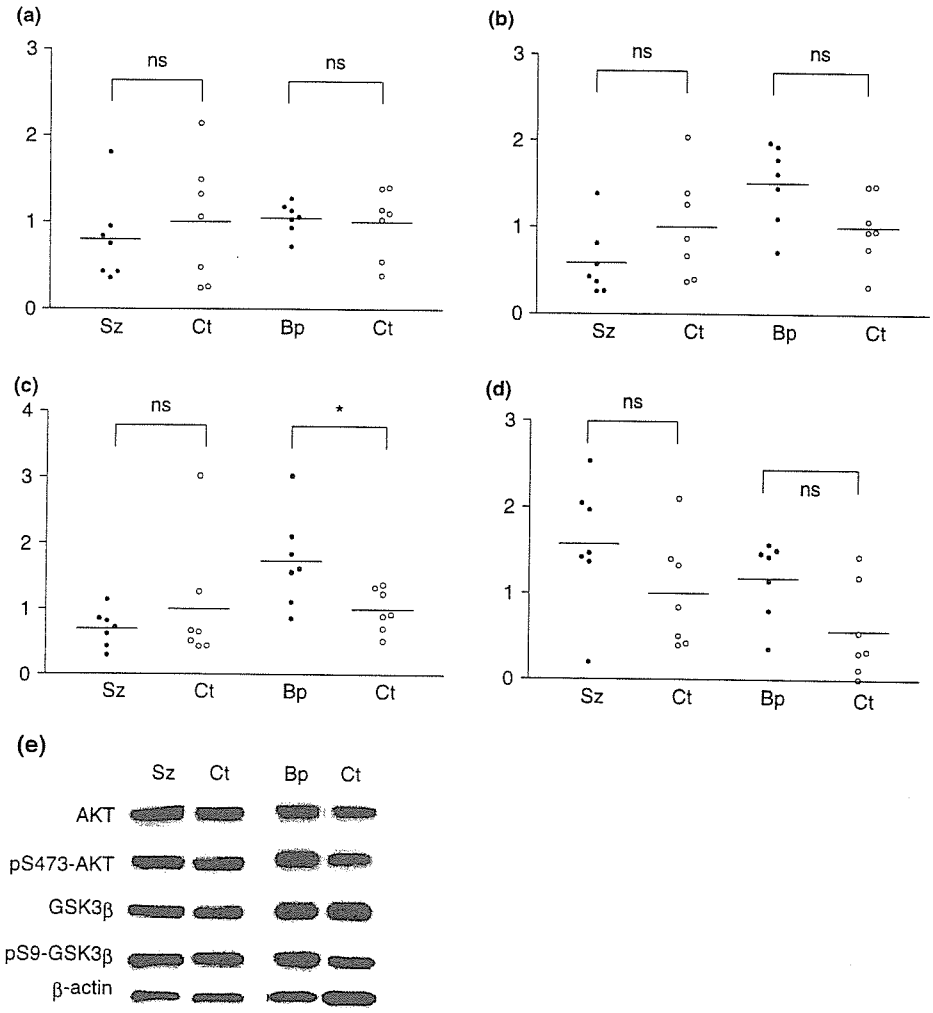

Fig. 1 Western blot analysis of protein expression and phosphorylation in cultured lymphocytes. (a) Relative expression levels of AKT against β-actin. (b) Relative expression levels of GSK3β against β-actin. (c) Phosphorylated fractions of AKT (p-Ser473-AKT) relative to total AKT. (d) Phosphorylated fractions of GSK3β (p-Ser9-GSK3β) relative to total GSK3β. The *y*-axis indicates the ratio of mean protein density from each disease group to the mean density value of corresponding control subjects. The mean value of each group is represented by a horizontal bar. Blots detected by chemiluminescence are shown in (e). Bp, bipolar disorder; Ct, control; Sz, schizophrenia; $^*p < 0.05$; ns, not-significant.

ratios of GSK3β (p-Ser9-GSK3β/total GSK3β) between psychiatric patients and controls (Fig. 1d). The phosphorylation level of AKT (p-Ser473-AKT/total AKT) was also not altered in schizophrenic patients ($p = 0.90$), but it was significantly increased in patients with bipolar disorder compared with controls ($p = 0.038$) (Fig. 1c).

AKT signaling in brain samples from the NSW TRC

Frontal cortex (BA9) postmortem samples from the first NSW TRC cohort were examined by western blotting to evaluate AKT signaling in schizophrenia samples. Tubulin was used as a marker because its expression remained stable in all brain samples. There were no significant differences in the expression levels and phosphorylation ratios of AKT, GSK3β (Fig. 2) and tau (Figs 3a and b) between the schizophrenia and control cases.

Given the fact that phosphorylated and therefore active AKT is a negative regulator of GSK3β, a direct phosporylator of tau, we speculated that an inverse correlation might exist between phosphorylation levels of AKT and tau. However, we found to the contrary significant positive, rather than negative, correlations between Ser473-phosphorylated AKT and Ser199-phosphorylated tau (Fig. 3c), and between Ser473-phosphorylated AKT and Ser396-phosphorylated tau (Fig. 3d). These results suggest that other, more salient, signal transduction pathways determine the phosphorylation status of AKT and/or tau in postmortem brains. AKT and tau are both dephosphorylated by protein phosphatase 2A (PP2A) (Goedert *et al.* 1992; Andjelkovic *et al.* 1996; Beaulieu *et al.* 2005). We previously reported that hypothermia induced by reduced glucose metabolism leads to tau hyperphosphorylation through the inactivation of PP2A (Planel *et al.* 2004). Hypoglycemia-hypothermia is one of the major agonal medical consequences. The precise mechanism for current findings on the phosphorylation status of AKT and tau is not known, but the involvement of factors relevant to terminal conditions, including phosphatase activities, should be further examined. In this regard, Li *et al.* (2004) reported a relationship between terminal medical conditions and the tissue pH of postmortem brains. We

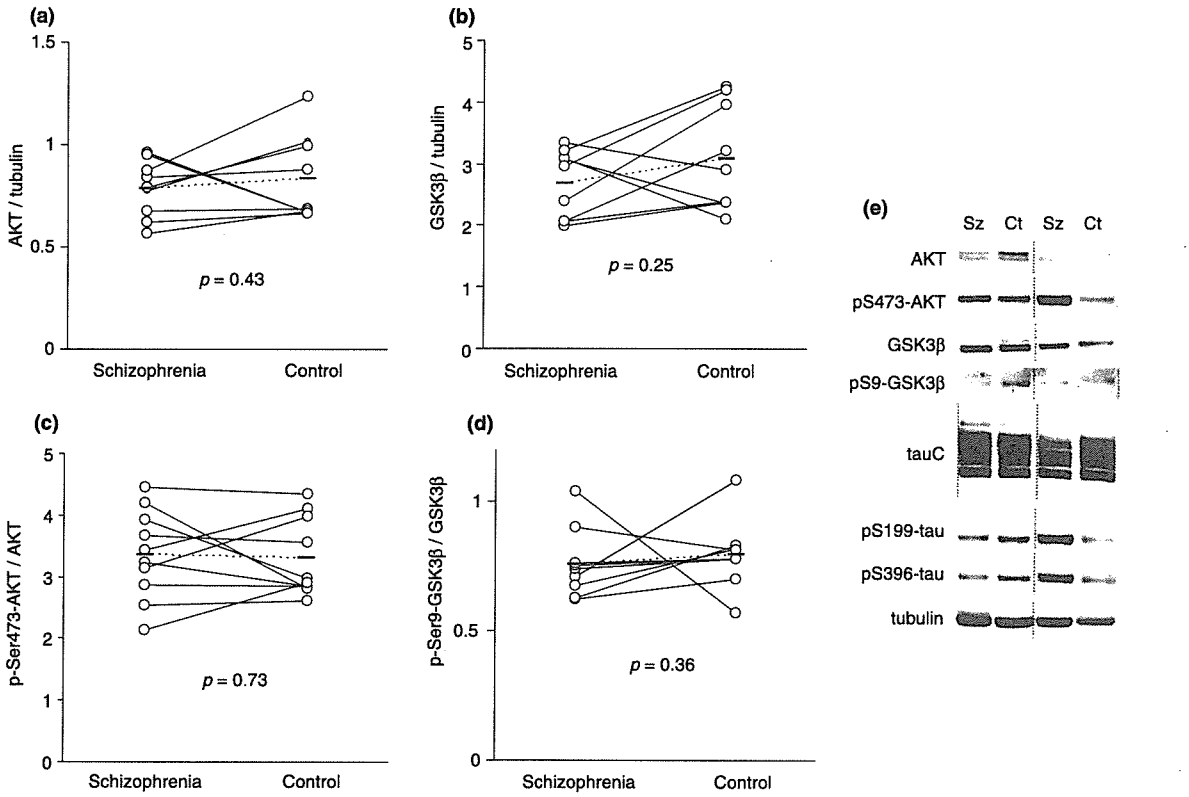

Fig. 2 Western blot analysis of protein expression and phosphorylation status in postmortem brains (BA9) of the first cohort from the NSW TRC (paired samples). (a) Relative expression levels of AKT against tubulin. (b) Relative expression levels of GSK3β against tubulin. (c) Phosphorylated fractions of AKT (p-Ser473-AKT) against total AKT. (d) Phosphorylated fractions of GSK3β (p-Ser9-GSK3β) against total GSK3β. Each age- and sex-matched pair is connected by a line, and the mean value of each group is indicated as a horizontal bar connected with dotted lines between the groups; the *p*-values are also shown. Blots were visualized by alkaline phosphatase staining (e). Ct, control; Sz, schizophrenia.

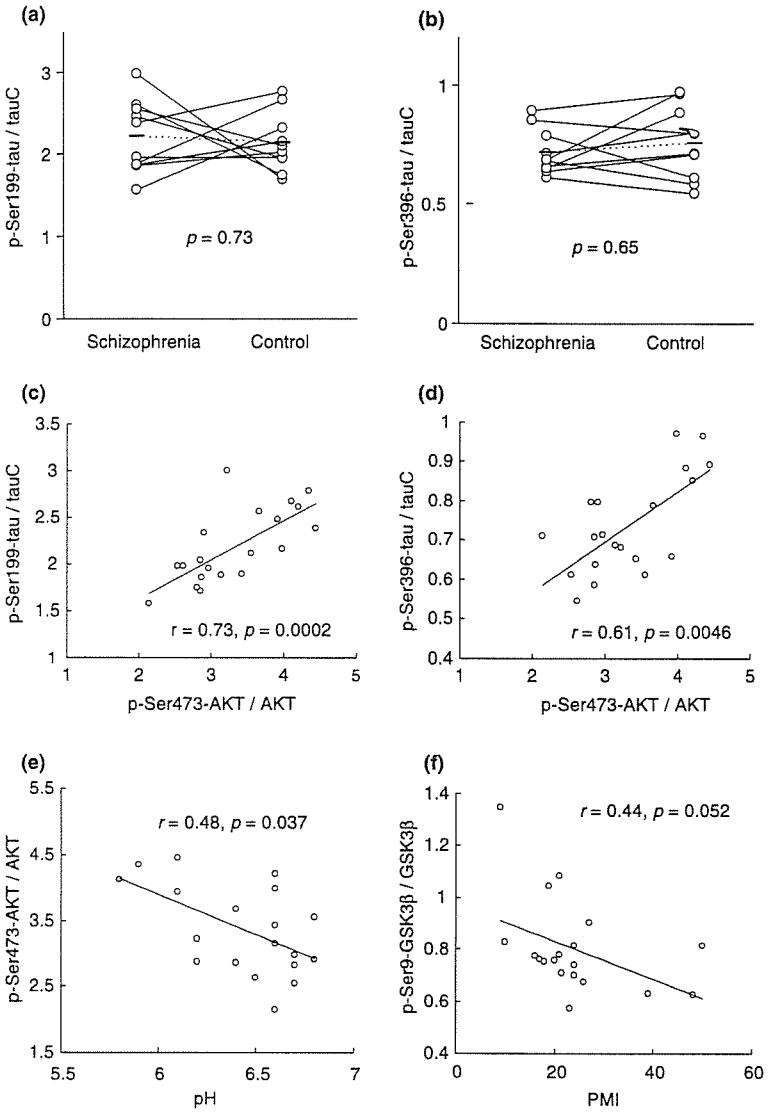

Fig. 3 Expression of phosphorylated tau and its correlation with phosphorylated AKT and GSKβ, and the effects of confounding factors on the expression of phosphorylated AKT and GSKβ, examined in postmortem brains (BA9) of the first NSW TRC cohort (paired samples). (a) Phosphorylated fractions of tau (p-Ser199-tau) against total tau (tauC). Each age- and sex-matched pair is connected by a line and the mean value of each group is indicated by a horizontal bar connected by dotted lines between groups; the *p*-value is also shown. (b) Phosphorylated fractions of tau (p-Ser396-tau) against total tau (tauC) are shown as in (a). (c) Correlation between the ratios of phosphorylated tau (p-Ser199-tau/TauC) and phosphorylated AKT (p-Ser473-AKT/AKT), examined in the combined schizophrenic and control samples. Spearman's correlation coefficient (r) and the *p*-value are shown. (d) Correlation between the ratio of phosphorylated tau (p-Ser396-tau/TauC) and phosphorylated AKT. (e) Effect of sample pH on the phosphorylation level of AKT (p-Ser473-AKT/AKT) in the combined schizophrenia and control samples. Spearman's correlation coefficient (r) and the *p*-value are shown. (f) Effect of postmortem interval (PMI) on the phosphorylation level of GSKβ (p-Ser9-GSKβ/GSKβ).

therefore examined the effects of pH and postmortem interval (PMI) on the phosphorylation level of proteins in brain samples. A significant inverse correlation was found between pH and AKT phosphorylation levels (Fig. 3e). An inverse correlation was also found between pH and tau phosphorylation at Ser199 ($r = -0.51$, $p = 0.025$, data not shown), and between pH and tau phosphorylation at Ser396 ($r = -0.22$, $p = 0.36$, data not shown), albeit not significant. For the effects of PMI on protein phosphorylation, GSK3β showed a tendency for inverse correlation with PMI (Fig. 3f). The phosphorylation levels of AKT and tau did not correlate with PMI (data not shown). Collectively, these data raise the point that the phosphorylation levels of AKT, GSK3β and tau in brain samples are largely dependent on the terminal medical state of the patient and the storage conditions after death.

We used anti-pan-AKT antibody to detect all subtypes of AKT proteins in the above experiments. Next, we focused on AKT1 subspecies using AKT1-specific antibodies in the second cohort of frontal cortex and hippocampus samples from the NSW TRC. No significant differences between schizophrenics and controls were observed in the expression levels of AKT1, GSKβ or phosphorylated GSK3β (Fig. 4).

AKT signaling in brain samples from the Stanley cohort

Emamian *et al.* (2004) analyzed frontal cortex samples (the anatomical subregions were not specified) obtained from the Stanley foundation and reported decreased AKT1 levels and reduced phosphorylated GSKβ in schizophrenics compared with controls. Therefore, we assessed the samples from the same resource. We also included the frontal cortex of individuals with bipolar disorder and major depression as

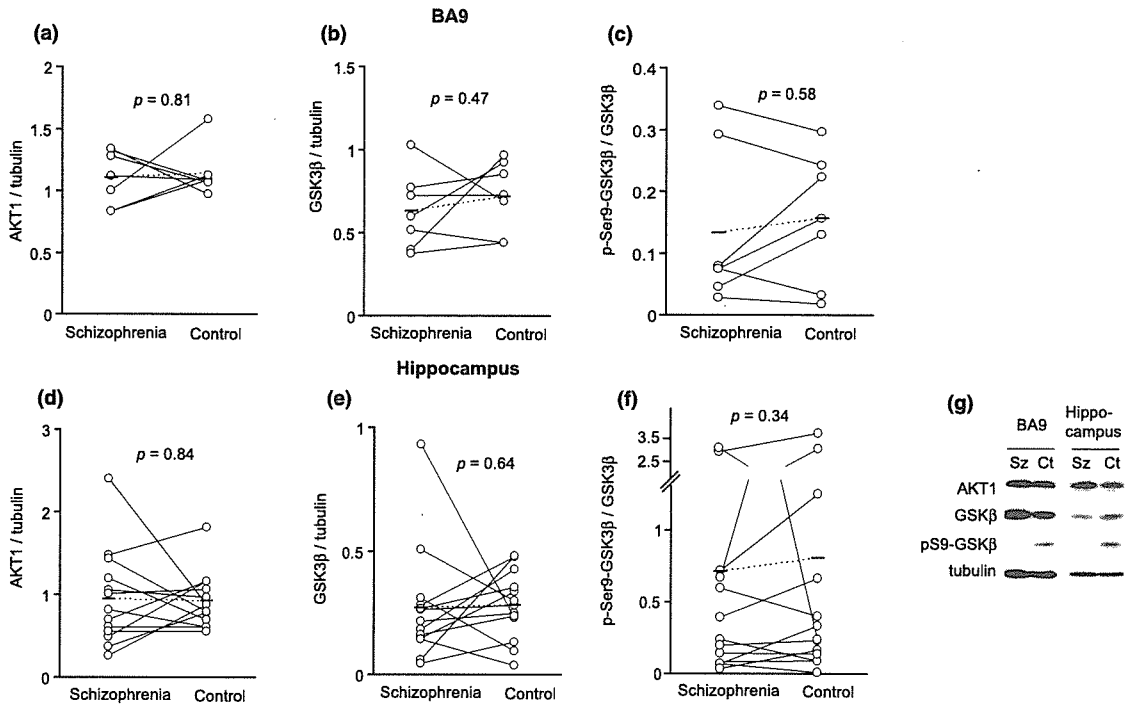

Fig. 4 Western blot analysis of protein expression and phosphorylation in postmortem brains (BA9, a, b and c; hippocampus, d, e and f) of the second NSW TRC cohort (paired samples). Panels (a) and (d) show the relative expression levels of AKT against tubulin. Panels (b) and (e) show the relative expression levels of GSK3β against tubulin. Panels (c) and (f) show the phosphorylated fractions of GSK3β (p-Ser9-GSK3β) against total GSK3β. Each age- and sex-matched pair is connected by a line and the mean value of each group is indicated by a horizontal bar connected by dotted lines between groups; the *p*-values are also shown. Blots detected by chemiluminescence are shown in (g). Ct, control; Sz, schizophrenia.

disease control groups, in addition to schizophrenia. The samples from schizophrenic and bipolar patients showed slightly, but not significantly, higher expression levels of AKT than in control subjects, whereas the expression in major depression samples did not differ from controls (Fig. 5a). No differences were found in the total GSK3β and the phosphorylation levels of GSK3β at Ser9 and tau at Ser199 between the three major psychiatric patients and control subjects (Figs 5b, c and d).

Discussion

In contrast to the report of Emamian *et al.* (2004), we were unable to detect an association between *AKT1* polymorphisms and schizophrenia in Japanese families with a predisposition to schizophrenia. Several other research groups have attempted replication studies, but the results vary among groups. Schwab *et al.* (2005) performed a family based association study using 79 Caucasian schizophrenia sib-pair families, an ethnic group similar to the original study. They investigated five SNPs used in the original study plus an additional two SNPs in the neighborhood of SNP3, and detected significant association with SNP3 ($p = 0.002$) and haplotypes ($p = 0.0013$) spanning the SNP3 locus. Their results replicate the association in Caucasians. In Japanese samples, Ikeda *et al.* (2004) reported a significant association between SNP5, but not SNP3, and haplotypes including SNP5 of *AKT1* and schizophrenia in case-control samples. Ohtsuki *et al.* (2004) also examined Japanese case-control samples, but could find no significant associations. In Taiwanese subjects, Liu *et al.* (2006) showed no significant association of the five SNPs with schizophrenia in a family based study. It is possible that *AKT1* polymorphisms confer a variable disease risk across different populations, with a strong contribution in Caucasians that falls to either equivocal or weak in East Asians. We have previously reported an association between *AKT1* and bipolar pedigrees in Caucasian samples (Toyota *et al.* 2003).

Our protein analyses failed to support the theory of decreased AKT expression in schizophrenia proposed by Emamian *et al.* (2004), as the expression levels of total AKT in schizophrenic brains from both the NSW TRC and the Stanley Bank were unchanged, and AKT1 levels in the second cohort of NSW TRC were also unaltered. One possible reason for the discrepancy may be a difference in the brain regions examined. We examined BA6 from the Stanley foundation and BA9 from the NSW TRC; both are areas of the frontal cortex. Emamian *et al.* (2004) did not specify the

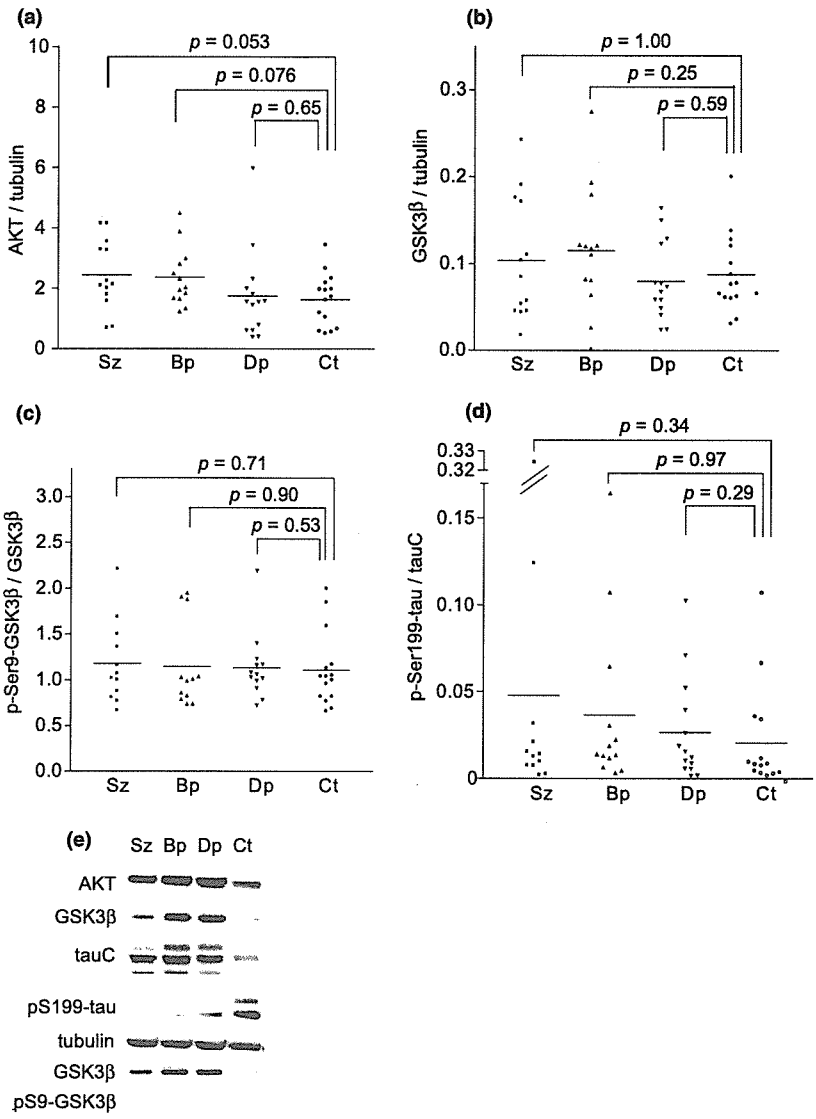

Fig. 5 Western blot analysis of protein expression and phosphorylation in postmortem brains (BA6) from the Stanley cohort. (a) Relative expression levels of AKT against tubulin. (b) Relative expression levels of GSK3β against tubulin. (c) Phosphorylated fractions of GSK3β (p-Ser9-GSK3β) against total GSK3β. (d) Phosphorylated fractions of tau (p-Ser119-tau) against total tau (tauC). The mean value of each group is indicated by a horizontal bar; the *p*-values are also shown. Blots were visualized by chemiluminescence (AKT, GSK3β, tauC, p-Ser199-tau and tubulin) and alkaline phosphatase staining (GSK3β and p-Ser9-GSK3β in the bottom two lines) (e). Bp, bipolar disorder; Ct, control; Dp, major depression; Sz, schizophrenia.

precise anatomical region used in their study and may have analyzed a different subarea of the frontal cortex. Our lymphocytes from Japanese schizophrenics did not display altered AKT levels. It is possible that reduced AKT expression in schizophrenia is not robust enough to be reliably detected across ethnic populations, anatomical regions and detailed experimental procedures including the selection of internal control probes.

Our examination of GSKβ from the brains and lymphocytes of schizophrenic subjects did not confirm the findings of Emamian *et al.* (2004). Importantly, it sounds a strong note of caution in the assessment of AKT brain phosphorylation levels, GSK3β and the downstream target tau. It is clear that the phosphorylation status of these proteins are affected by numerous factors that are difficult to control in postmortem specimens, such as temperature, the period of brain dissection and preservation, PMI and pH. Indeed, several lines of evidence have suggested that the phosphorylation status of GSK3β in postmortem brains does not reflect that of the living brain. For example, Li *et al.* (2005) found that in the mouse brain, approximately 90% of both phospho-Ser-GSK3α and β were dephosphorylated within 2 min of decapitation. This is in keeping with our failure to detect phosphorylated GSK3β at Ser9 in brain samples using standard chemiluminescent methods. Furthermore, a number of reports have shown that GSK3β phosphorylation status and function are controlled by circadian rhythms (Martinek *et al.* 2001; Iitaka *et al.* 2005).

Before the report of Emamian *et al.* (2004), GSK3β was implicated in the neurodevelopmental disturbances of schizophrenia. Taking the opposite stand, Kozlovsky *et al.* (2002) postulated that reduced activity of GSK3β could

contribute to the pathogenesis of schizophrenia, based on their findings that schizophrenic postmortem brains showed reduced expression levels of GSK3β mRNA and protein. On the other hand, Beasley *et al.* (2002) did not observe a reduction of GSK3β protein levels in schizophrenia.

In conclusion, although the newly proposed theory of reduced signaling in the AKT-GSK3β molecular cascade may explain some aspects of schizophrenia pathology, more evidence is required, particularly regarding the *in vivo* phosphorylation levels of constituent proteins directly linked to the functional status of the signaling cascade.

Acknowledgements

This work was supported by research grants from RIKEN Brain Science Institute and a Grant-in-Aid for Scientific Research (Japanese Ministry of Education, Culture, Sports, Science and Technology). The NSW TRC tissues were received from the Australian Brain Donor Programs NSW Tissue Resource Centre, which is supported by the University of Sydney, National Health and Medical Research Council of Australia, Neuroscience Institute of Schizophrenia and Allied Disorders, National Institute of Alcohol Abuse and Alcoholism and NSW Department of Health. Postmortem brains were donated by The Stanley Medical Research Institute's Brain Collection, courtesy of Drs Knable, Torrey, Webster, Weis and Yolken.

References

American Psychiatric Association (1994) Diagnostic and statistical manual of mental disorders, 4th edn (DSM-IV). American Psychiatric Association, Washington DC.

Andjelkovic M., Jakubowicz T., Cron P., Ming X. F., Han J. W. and Hemmings B. A. (1996) Activation and phosphorylation of a pleckstrin homology domain containing protein kinase (RAC-PK/PKB) promoted by serum and protein phosphatase inhibitors. *Proc. Natl Acad. Sci. USA* **93**, 5699–5704.

Aoki-Suzuki M., Yamada K., Meerabux J. *et al.* (2005) A family-based association study and gene expression analyses of netrin-G1 and -G2 genes in schizophrenia. *Biol. Psychiatry* **57**, 382–393.

Barbeau D., Liang J. J., Robitalille Y., Quirion R. and Srivastava L. K. (1995) Decreased expression of the embryonic form of the neural cell adhesion molecule in schizophrenic brains. *Proc. Natl Acad. Sci. USA* **92**, 2785–2789.

Beasley C., Cotter D. and Everall I. (2002) An investigation of the Wnt-signalling pathway in the prefrontal cortex in schizophrenia, bipolar disorder and major depressive disorder. *Schizophr. Res.* **58**, 63–67.

Beaulieu J. M., Sotnikova T. D., Yao W. D., Kockeritz L., Woodgett J. R., Gainetdinov R. R. and Caron M. G. (2004) Lithium antagonizes dopamine-dependent behaviors mediated by an AKT/glycogen synthase kinase 3 signaling cascade. *Proc. Natl Acad. Sci. USA* **101**, 5099–5104.

Beaulieu J. M., Sotnikova T. D., Marion S., Lefkowitz R. J., Gainetdinov R. R. and Caron M. G. (2005) An Akt/beta-arrestin 2/PP2A signaling complex mediates dopaminergic neurotransmission and behavior. *Cell* **122**, 261–273.

Beffert U., Morfini G., Bock H. H., Reyna H., Brady S. T. and Herz J. (2002) Reelin-mediated signaling locally regulates protein kinase B/Akt and glycogen synthase kinase 3beta. *J. Biol. Chem.* **277**, 49 958–49 964.

Clayton D. (1999) A generalization of the transmission/disequilibrium test for uncertain-haplotype transmission. *Am. J. Hum. Genet.* **65**, 1170–1177.

Conti L., Sipione S., Magrassi L. *et al.* (2001) Shc signaling in differentiating neural progenitor cells. *Nat. Neurosci.* **4**, 579–586.

Cross D. A., Alessi D. R., Cohen P., Andjelkovich M. and Hemmings B. A. (1995) Inhibition of glycogen synthase kinase-3 by insulin mediated by protein kinase B. *Nature* **378**, 785–789.

De Ferrari G. V., Chacón M. A., Barría M. I., Garrido J. L., Godoy J. A., Olivares G., Reyes A. E., Alvarez A., Bronfman M. and Inestrosa N. C. (2003) Activation of Wnt signaling rescues neurodegeneration and behavioral impairments induced by beta-amyloid fibrils. *Mol. Psychiatry* **8**, 195–208.

Dudbridge F. (2003) Pedigree disequilibrium tests for multilocus haplotypes. *Genet. Epidemiol.* **25**, 115–121.

Dudek H., Datta S. R., Franke T. F., Birnbaum M. J., Yao R., Cooper G. M., Segal R. A., Kaplan D. R. and Greenberg M. E. (1997) Regulation of neuronal survival by the serine-threonine protein kinase Akt. *Science* **275**, 661–665.

Emamian E. S., Hall D., Birnbaum M. J., Karayiorgou M. and Gogos J. A. (2004) Convergent evidence for impaired AKT1-GSK3beta signaling in schizophrenia. *Nat. Genet.* **36**, 131–137.

Goedert M., Cohen E. S., Jakes R. and Cohen P. (1992) p42 MAP kinase phosphorylation sites in microtubule-associated protein tau are dephosphorylated by protein phosphatase 2A1. Implications for Alzheimer's disease. *FEBS Lett.* **312**, 95–99.

Iitaka C., Miyazaki K., Akaike T. and Ishida N. (2005) A role for glycogen synthase kinase-3beta in the mammalian circadian clock. *J. Biol. Chem.* **280**, 29 397–29 402.

Ikeda M., Iwata N., Suzuki T., Kitajima T., Yamanouchi Y., Kinoshita Y., Inada T. and Ozaki N. (2004) Association of AKT1 with schizophrenia confirmed in a Japanese population. *Biol. Psychiatry* **56**, 698–700.

Ilia M., Beasley C., Meijer D., Kerwin R., Cotter D., Everall I. and Price J. (2002) Expression of Oct – 6, a POU III domain transcription factor, in schizophrenia. *Am. J. Psychiatry* **159**, 1174–1182.

Impagnatiello F., Guidotti A. R., Pesold C. *et al.* (1998) A decrease of reelin expression as a putative vulnerability factor in schizophrenia. *Proc. Natl Acad. Sci. USA* **95**, 15 718–15 723.

Ishiguro K., Sato K., Takamatsu M., Park J., Uchida T. and Imahori K. (1995) Analysis of phosphorylation of tau with antibodies specific for phosphorylation sites. *Neurosci. Lett.* **202**, 81–84.

Keks N., Hill C., Opeskin K., Copolov D. and Dean B. (1999) Psychiatric diagnosis after death: the problems of accurate diagnosis. in *The Use of CNS Autopsy Tissue in Psychiatric Research: a Practical Guide* (Dean B., Hyde T. M. and Kleinman J., eds.), pp. 19–37. Gordon and Breach Science Publishers, Sydney.

Kozlovsky N., Belmaker R. H. and Agam G. (2000) Low GSK-3beta immunoreactivity in postmortem frontal cortex of schizophrenic patients. *Am. J. Psychiatry* **157**, 831–833.

Kozlovsky N., Belmaker R. H. and Agam G. (2002) GSK-3 and the neurodevelopmental hypothesis of schizophrenia. *Eur. Neuropsychopharmacol.* **12**, 13–25.

Kozlovsky N., Shanon-Weickert C., Tomaskovic-Crook E., Kleinman J. E., Belmaker R. H. and Agam G. (2004) Reduced GSK-3beta mRNA levels in postmortem dorsolateral prefrontal cortex of schizophrenic patients. *J. Neural. Transm.* **111**, 1583–1592.

Li J. Z., Vawter M. P., Walsh D. M. *et al.* (2004) Systematic changes in gene expression in postmortem human brains associated with tissue pH and terminal medical conditions. *Hum. Mol. Genet.* **13**, 609–616.

Li X., Friedman A. B., Roh M. S. and Jope R. S. (2005) Anesthesia and post-mortem interval profoundly influence the regulatory serine phosphorylation of glycogen synthase kinase-3 in mouse brain. *J. Neurochem.* **92**, 701–704.

Liu Y. L., Fann C. S., Liu C. M. *et al.* (2006) Absence of significant associations between four AKT1 SNP markers and schizophrenia in the Taiwanese population. *Psychiatr. Genet.* **16**, 39–41.

Markus A., Zhong J. and Snider W. D. (2002) Raf and akt mediate distinct aspects of sensory axon growth. *Neuron* **35**, 65–76.

Martin E. R., Monks S. A., Warren L. L. and Kaplan N. L. (2000) A test for linkage and association in general pedigrees: the pedigree disequilibrium test. *Am. J. Hum. Genet.* **67**, 146–154.

Martinek S., Inonog S., Manoukian A. S. and Young M. W. (2001) A role for the segment polarity gene shaggy/GSK-3 in the Drosophila circadian clock. *Cell* **105**, 769–779.

Morishima-Kawashima M., Hasegawa M., Takio K., Suzuki M., Yoshida H., Titani K. and Ihara Y. (1995) Proline-directed and non-proline-directed phosphorylation of PHF-tau. *J. Biol. Chem.* **270**, 823–829.

O'Connell J. R. and Weeks D. E. (1998) PedCheck: a program for identification of genotype incompatibilities in linkage analysis. *Am. J. Hum. Genet.* **63**, 259–266.

Ohnuma T., Kato H., Arai H., McKenna P. J. and Emson P. C. (2003) Expression of Fyn, a non-receptor tyrosine kinase in prefrontal cortex from patients with schizophrenia and its correlation with clinical onset. *Brain Res. Mol. Brain Res.* **112**, 90–94.

Ohtsuki T., Inada T. and Arinami T. (2004) Failure to confirm association between AKT1 haplotype and schizophrenia in a Japanese case-control population. *Mol. Psychiatry* **9**, 981–983.

Planel E., Miyasaka T., Launey T., Chui D. H., Tanemura K., Sato S., Murayama O., Ishiguro K., Tatebayashi Y. and Takashima A. (2004) Alterations in glucose metabolism induce hypothermia leading to tau hyperphosphorylation through differential inhibition of kinase and phosphatase activities: implications for Alzheimer's disease. *J. Neurosci.* **24**, 2401–2411.

Sato S., Tatebayashi Y., Akagi T. *et al.* (2002) Aberrant tau phosphorylation by glycogen synthase kinase-3beta and JNK3 induces oligomeric tau fibrils in COS-7 cells. *J. Biol. Chem.* **277**, 42 060–42 065.

Schwab S. G., Hoefgen B., Hanses C., Hassenbach M. B., Albus M., Lerer B., Trixler M., Maier W. and Wildenauer D. B. (2005) Further evidence for association of variants in the AKT1 gene with schizophrenia in a sample of European sib-pair families. *Biol. Psychiatry* **58**, 446–450.

Sham P. C. and Curtis D. (1995) Monte Carlo tests for associations between disease and alleles at highly polymorphic loci. *Ann. Hum. Genet.* **59**, 97–105.

Takahashi M., Shirakawa O., Toyooka K. *et al.* (2000) Abnormal expression of brain-derived neurotrophic factor and its receptor in the corticolimbic system of schizophrenic patients. *Mol. Psychiatry* **5**, 293–300.

Torrey E. F., Webster M., Knable M., Johnston N. and Yolken R. H. (2000) The stanley foundation brain collection and neuropathology consortium. *Schizophr. Res.* **44**, 151–155.

Toyota T., Yamada K., Detera-Wadleigh S. D. and Yoshikawa T. (2003) Analysis of a cluster of polymorphisms in AKT1 gene in bipolar pedigrees: a family-based association study. *Neurosci. Lett.* **339**, 5–8.

Weinberger D. R. (1996) On the plausibility of 'the neurodevelopmental hypothesis' of schizophrenia. *Neuropsychopharmacology* **14**, 1S–11S.

Yamada K., Iwayama-Shigeno Y., Yoshida Y., Toyota T., Itokawa M., Hattori E., Shimuzu H. and Yoshikawa T. (2004) Family-based association study of schizophrenia with 444 markers and analysis of a new susceptibility locus mapped to 11q13.3. *Am. J. Med. Genet.* **127B**, 11–19.

ELSEVIER

Neurobiology of Disease

www.elsevier.com/locate/ynbdi
Neurobiology of Disease 24 (2006) 334–344

Loss of M_5 muscarinic acetylcholine receptors leads to cerebrovascular and neuronal abnormalities and cognitive deficits in mice

Runa Araya,[a,1] Takanori Noguchi,[b,1] Munehiro Yuhki,[a] Naohito Kitamura,[a] Makoto Higuchi,[c] Takaomi C. Saido,[c] Kenjiro Seki,[b] Shigeyoshi Itohara,[b] Masako Kawano,[d] Kentaro Tanemura,[e] Akihiko Takashima,[e] Kazuyuki Yamada,[f] Yasushi Kondoh,[g] Iwao Kanno,[g] Jürgen Wess,[h] and Masahisa Yamada[a,*]

[a]*Yamada Research Unit, RIKEN Brain Science Institute, Saitama 351-0198, Japan*
[b]*Laboratory for Behavioral Genetics, RIKEN Brain Science Institute, Saitama 351-0198, Japan*
[c]*Laboratory for Proteolytic Neuroscience, RIKEN Brain Science Institute, Saitama 351-0198, Japan*
[d]*Laboratory for Cell Culture Development, RIKEN Brain Science Institute, Saitama 351-0198, Japan*
[e]*Laboratory for Alzheimer's Diseases, RIKEN Brain Science Institute, Saitama 351-0198, Japan*
[f]*Advanced Technology Development Group/Research Resources Center, RIKEN Brain Science Institute, Saitama 351-0198, Japan*
[g]*Department of Radiology and Nuclear Medicine, Akita Research Institute of Brain and Blood Vessels, Akita 010-0874, Japan*
[h]*Laboratory of Bioorganic Chemistry, National Institute of Diabetes and Digestive and Kidney Diseases, Bethesda, Maryland 20892, USA*

Received 28 March 2006; revised 13 June 2006; accepted 17 July 2006
Available online 7 September 2006

The M_5 muscarinic acetylcholine receptor (M5R) has been shown to play a crucial role in mediating acetylcholine-dependent dilation of cerebral blood vessels. We show that male $M5R^{-/-}$ mice displayed constitutive constriction of cerebral arteries using magnetic resonance angiography in vivo. Male $M5R^{-/-}$ mice exhibited a significantly reduced cerebral blood flow (CBF) in the cerebral cortex, hippocampus, basal ganglia, and thalamus. Cortical and hippocampal pyramidal neurons from $M5R^{-/-}$ mice showed neuronal atrophy. Hippocampus-dependent spatial and nonspatial memory was also impaired in $M5R^{-/-}$ mice. In $M5R^{-/-}$ mice, CA3 pyramidal cells displayed a significantly attenuated frequency of the spontaneous postsynaptic current and long-term potentiation was significantly impaired at the mossy fiber-CA3 synapse. Our findings suggest that impaired M5R signaling may play a role in the pathophysiology of cerebrovascular deficits. The M_5 receptor may represent an attractive novel therapeutic target to ameliorate memory deficits caused by impaired cerebrovascular function.

Keywords: Cognition; Cerebral blood flow; Muscarinic acetylcholine receptor; Neuronal atrophy

Introduction

A considerable body of evidence indicates that disturbances in the central muscarinic acetylcholine (ACh) receptor system play a role in several pathophysiologic conditions, including Alzheimer's and Parkinson's disease, depression, schizophrenia, and epilepsy (Wess, 2004). Degeneration of cholinergic neurons in the basal forebrain is central to the pathogenesis of Alzheimer's disease and occurs early in the disease process (Davies and Maloney, 1976; Coyle et al., 1983; Bartus, 2000). Muscarinic ACh receptors are abundantly expressed in forebrain areas thought to be important for cognitive functions, such as the cerebral cortex and hippocampus (Davies and Maloney, 1976; Levey, 1996). Recent studies with muscarinic receptor knockout mice have revealed distinct CNS functions for the individual muscarinic receptor subtypes (M_1–M_5) (Wess et al., 2003; Wess, 2004).

It has been hypothesized that impairments in cerebrovascular function involving, among other mechanisms, vascular muscarinic cholinergic pathways may play a role in the progress of Alzheimer's dementia (Iadecola, 2003, 2004). Activation of cholinergic basal forebrain neurons plays an important role in the regulation of cerebral vascular resistance, relaxation and contraction of blood vessels, and regional blood flow (Gomi et al., 1991; Faraci and Sigmund, 1999; Hotta et al., 2002; Sato et al., 2004; Hamel, 2004). Therefore, reduced signaling through both neuronal and vascular muscarinic receptors may contribute to the pronounced memory deficits associated with Alzheimer's disease. An immunohistochemical study suggested that M_5 receptors (M5R) are expressed by

* Corresponding author. Fax: +81 48 467 7648.
E-mail address: masahisa@brain.riken.jp (M. Yamada).
[1] These authors contributes equally to this work.
Available online on ScienceDirect (www.sciencedirect.com).

0969-9961/$ - see front matter © 2006 Elsevier Inc. All rights reserved.
doi:10.1016/j.nbd.2006.07.010

endothelial cells of the circle of Willis and cerebral arteries (Tayebati et al., 2003). Moreover, we reported previously that ACh-mediated vasodilation of cerebral arteries and arterioles was absent in M_5 receptor-deficient mice ($M5R^{-/-}$ mice) (Yamada et al., 2001a). Taken together, these observations suggest that M_5 receptors located on vascular endothelial cells mediate the vasorelaxing effects of ACh on cerebral blood vessels. We therefore hypothesized that the permanent lack of M_5 receptors may cause cerebrovascular insufficiencies, potentially associated with impaired neuronal function and cognitive deficits.

Here we show that $M5R^{-/-}$ mice display constitutive constriction of cerebral arteries using magnetic resonance angiography (MRA) in vivo. We observed a significantly reduced CBF in the cerebral cortex, hippocampus, basal ganglia, and thalamus of $M5R^{-/-}$ mice. In hippocampal pyramidal neurons, these changes were associated with a reduction in the number of spines, dendritic atrophy, and a decrease in spontaneous excitatory activity. Moreover, hippocampus-dependent memory was also found to be impaired in $M5R^{-/-}$ mice. These results strongly suggest that M_5 receptors are required for proper cerebrovascular and neuronal function. The M_5 receptor may represent an attractive novel therapeutic target to ameliorate memory deficits caused by impaired cerebrovascular function.

Materials and methods

Animals

$M1R^{-/-}$ mice (Fisahn et al., 2002), $M3R^{-/-}$ mice (Yamada et al., 2001b), and $M5R^{-/-}$ mice (Yamada et al., 2001a) were produced as described previously. Gene disruption resulted in nonfunctional muscarinic receptors in each case. All studies were carried out with male mice. In each study, wild-type and mutant mice were age-matched. Unless stated otherwise, all experiments were carried out with littermates (C57BL6/J × 129 SvEv hybrids) of the F4–F5 generation. To generate congenic $M5R^{-/-}$ mice, we backcrossed $M5R^{-/-}$ mice for 10 generations onto the C57BL6/J mouse background. The congenic mice were used for behavioral tests. Animal experiments were approved by the Animal Experiment Committee of the RIKEN Brain Science Institute.

MRA analysis

Mice were anesthetized with pentobarbital and subjected to micro-MRI scans using a vertical bore 9.4 T Bruker AVANCE 400WB imaging spectrometer with a 250 mT/m actively shielded microimaging gradient insert (Bruker BioSpin GmbH, Ettlingen, Germany) (Higuchi et al., 2005). A 25-mm resonator was used for signal excitation and detection. The depth of anesthesia was monitored with a breathing sensor, and was maintained with 0.5 to 1.5% isoflurane in air (2 l/min flow rate). Two-dimensional horizontal MRA images were acquired by using a method derived from gradient-echo pulse sequence with flow compensation. The scans were performed with the following imaging parameters: TR=30 ms; TE=4.7 ms; flip angle=85°; matrix=256×256; field of view=2×2 cm^2; number of slices=40; slice thickness=0.2 mm; and total imaging time=51 min (10 averages). Angiograms were obtained by generating maximum intensity projections using a Paravision software (Bruker BioSpin GmbH).

Arterial vascular diameter was measured in the basilar artery and proximal and distal portions of the MCA. Starting points (SPs) and ending points (EPs) for measurements were designated as follows: SP, 0.5 mm distal to the beginning of the artery, EP, 3.5 mm distal to SP (basilar artery); SP, 0.5 mm distal to the beginning of the artery, EP, 1.5 mm distal to SP (proximal MCA); and SP, 4 mm distal to the beginning of the artery, EP, 1.5 mm distal to SP (distal MCA). The SPs and EPs are indicated in Fig. 1. Subsequently, the area of the segment ranging from the SP to the EP on each arterial portion was measured on the longitudinal projection of the vessel, and mean vascular diameter was determined as the ratio of the measured area to the length of the segment.

Morphometric investigations of living brains were conducted for WT and $M5R^{-/-}$ mice at the age of 12 months (N=5 in each group) using a Bruker AVANCE 400WB imaging spectrometer. Signal excitation and detection were performed by using a 25-mm resonator. T1-weighted 2D gradient-echo (field of view=20×20 mm^2, matrix dimensions=256×256, nominal in-plane resolution=78 μm×78 μm, slice thickness=1 mm, number of slices=15, TE=2.5 ms, TR=250 ms, flip angle=85°, number of averages=15, total imaging time=16 min) MR scans were performed. The volume of the whole brain was determined by using a PMOD software (PMOD Technologies, Zurich, Switzerland).

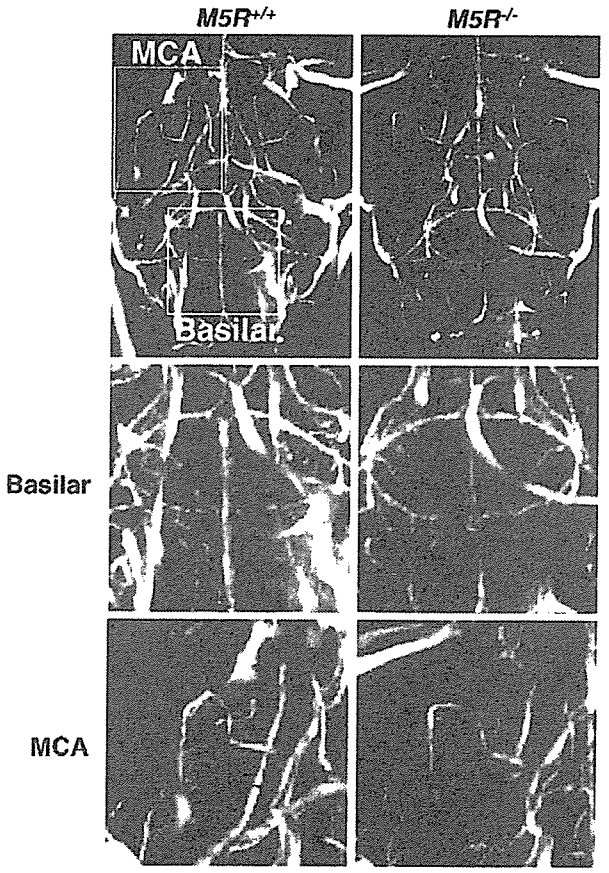

Fig. 1. Representative angiograms of the basilar artery and the middle cerebral artery (MCA) from $M5R^{-/-}$ and $M5R^{-/-}$ mice. High-resolution magnetic resonance angiography (MRA) was used as a means to investigate the arterial cerebrovascular hemodynamics noninvasively in adult mice. The adjacent vessels emerging from the basilar artery and the MCA are highlighted. $M5R^{-/-}$ mice showed reduced diameters of the basilar artery and MCA. Arrows indicate the blood vessel regions that were measured for vessel diameter (quantitative data are given in Fig. 2). p, proximal; d, distal.

CBF monitoring

Animals were prepared for the measurement of local CBF by quantitative autoradiography. Local CBF was measured using ^{14}C-labeled iodoantipyrine (IAP) as a tracer, as described elsewhere (Jay et al., 1988). ^{14}C-labeled IAP (Amersham, 5 μCi in 100 μl of physiologic saline) was infused intravenously, and timed arterial samples were collected. For determination of tissue ^{14}C concentrations, serial sections (20 μm) were cut using a cryostat, mounted on glass slides, and exposed to X-ray film (type OM1, Kodak Co.), together with calibrated ^{14}C standards. The ^{14}C concentration (nCi/g) of regions of interest was determined using MATLAB. CBF (ml/100 g/min) was calculated using a previously described equation (Sakurada et al., 1978).

Measurements of arteriole diameter and CBF using a laser Doppler flowmeter

Measurements of arteriole diameter and CBF were performed as previously described (Noguchi et al., 1999). Mice were initially anesthetized with a mixture of ketamine (200 mg/kg, i.p.) and xylazine (10 mg/kg, i.p.) and were allowed to breath freely. The animals were fixed in a stereotaxic frame, with the bone overlying the dorsal surface positioned at the center of the left parietal bone. The animal in the stereotaxic frame was placed on the stage of a microscope equipped with a long-working-distance objective, and the MCA (A1 level) was monitored with a charge-coupled device (CCD) camera, and images were captured on a personal computer. The branches of the MCA were defined in the order from A1 to A3 (for classification scheme, see Refs. Horton, 1945; Fenton and Zweifah, 1981). A probe with a diameter of 0.5 mm was attached to the point of divergence of the MCA, and CBF was measured continuously in the parietal lobe using a laser Doppler flowmeter (ALF 21, Advance Co., Ltd., Tokyo), in conjunction with a PowerLab system (AD Instruments, CA, USA). After measuring CBF and vessel diameter, blood samples (30 μl) were obtained from the abdominal aorta to measure the levels of arterial blood gases (Pao_2, $Paco_2$) and pH (Blood Gas Analyzer 248, Bayer Medical, Medford, MA, USA). We did not observe any significant differences in blood gas levels or pH between $M5R^{-/-}$ and $M5R^{+/+}$ mice (data not shown).

Serum nitrate concentration

A microanalytical gas chromatographic (GC) method for the analysis of nitrate in mouse serum was performed basically as described (Dunphy et al., 1990). Reaction products were extracted by mixing with n-hexane. An aliquot (2 μl) of the n-hexane solution was injected into a GC-MS system. GC-MS was carried out on a Hewlett-Packard HP 5790A gas chromatograph (Palo Alto, CA, USA) interfaced to a JEOL JMS SX-102A mass spectrometer (Tokyo, Japan). The column was a J and W fused-silica capillary tube of DB-1 (30 m×0.32 mm I.D., 0.25-μm film thickness). Mesitylene derivatives of unlabeled and ^{15}N-labeled nitrate had practically identical retention times (about 3.7 min).

Western blotting

Mouse brain homogenates were prepared as previously described (Planel et al., 2001). We used the following primary antibodies: NR1 (BD PharMingen), GluR1 (Chemicon), and GluR5 (Upstate).

Histologic analysis

For Golgi staining, mice were anesthetized with pentobarbital and perfused with 10% formaldehyde neutral buffer. The brains were removed and postfixed for 6 h. Subsequently, pieces of tissue were immersed in Golgi solution (3.15% potassium dichromate, 0.2% osmium) for 5 days. Tissue was immersed in 0.75% silver nitrate for 24 h. Golgi-impregnated dendritic segments selected for analysis were located 100 to 250 μm from the pyramidal cell bodies in the fifth cortical layer.

Electrophysiologic recording

Slice preparation and recording

Slice preparations and solutions were made as previously described (Kamiya et al., 2002). Male mice (6 months old) were used throughout these experiments. After a mouse was deeply anesthetized with ether, it was immersed in ice-cold water except for the nose for 3 min to reduce brain temperature. Immediately after decapitation, the brain was removed and placed in an ice-cold artificial medium gassed with 95% O_2 and 5% CO_2. The composition of the medium was as follows (in mM): sucrose 250, KCl 5, NaH_2PO_4 1.24, $MgSO_4$ 10, $CaCl_2$ 0.5, $NaHCO_3$ 26, and glucose 10. Transverse slices (350–400 μm) from the hippocampus, including the entorhinal cortex, were prepared from both hemispheres with a microslicer (DTK-2000; Dosaka, Osaka, Japan). The obtained hippocampal slices were incubated in an artificial medium (composition in mM: NaCl 124, KCl 5, NaH_2PO_2 1.24, $MgSO_4$ 1.0, $CaCl_2$ 2.0, $NaHCO_3$ 26 and glucose 10) at room temperature (25°C) for at least 1 h before recording. Slices were then transferred to a recording chamber and submerged in artificial cerebrospinal fluid (aCSF). Recordings were done at room temperature. During recording, the slices were continuously perfused with oxygenated medium at a flow rate of 1 ml/min. Extracellular fEPSPs were amplified and filtered at 2 kHz and sampled at 50 kHz with an Axopatch 200B patch clamp amplifier (Axon Instruments). Data were acquired with Clampex8 and analyzed with Clampfit 7 (Axon Instruments) for off-line analysis. The initial slope and amplitude of the fEPSPs at half of their peak were measured.

Whole-cell patch clamp recording

Whole-cell patch recording from hippocampal CA3 pyramidal neurons was performed as previously described (Seki et al., 2001), using borosilicate electrodes containing (in mM) KCl 120, K-gluconate 20, NaCl 8, HEPES 10, EGTA 0.5, $MgCl_2$ 1, Na-ATP 4, Na-GTP 1, and sucrose 16, with the pH adjusted to 7.2 with NaOH. The resistance of the recording electrode was 11 to 13 MΩ. The electrode was inserted into the CA3 pyramidal cell layer monitored via an infrared-CCD (IR-CCD) camera (40× water immersion lens). Approximately 10 to 30 mm Hg positive pressure was applied to the pipette during insertion. After a sudden increase in access resistance of the electrode, the positive pressure on the electrode was removed in a blind slice patch manner. In successful cases, the access resistance and membrane potential continuously decreased for approximately 5 min before stabilizing. Intracellular potentials were amplified 10 times with an Axopatch 200B. Membrane resistance and resting membrane potential were measured. Neurons showed a resting membrane potential of less than −65 mV. The resting membrane potentials and series resistance values in the studied neurons ranged from −73 to −67 mV and from 36 to 58 MΩ, respectively. Postsynaptic currents were filtered at 1 kHz and sampled